On the Use of Mega Constellation Services in Space: Integrating LEO Platforms into 6G Non-Terrestrial Networks

Gabriel Maiolini Capez, Mauricio A Cáceres, Roberto Armellin, Chris P Bridges, Juan A Fraire, Stefan Frey, Roberto Garello

On the Use of Mega Constellation Services in Space: Integrating LEO Platforms into 6G Non-Terrestrial Networks

Gabriel Maiolini Capez, *Graduate Student Member, IEEE,* Mauricio A. Cáceres, Roberto Armellin, Chris P. Bridges, *Member, IEEE,* Juan A. Fraire, *Senior Member, IEEE,* Stefan Frey, Roberto Garello, *Senior Member, IEEE*

***Abstract*—This paper presents a framework for integrating Low-Earth Orbit (LEO) platforms with Non-Terrestrial Networks (NTNs) in the emerging 6G communication landscape. Our work applies the Mega-Constellation Services in Space (MCSS) paradigm, leveraging LEO mega-constellations' expansive coverage and capacity, designed initially for terrestrial devices, to serve platforms in lower LEO orbits. Results show that this approach overcomes the limitation of sporadic and time-bound satellite communication links, a challenge not fully resolved by available Ground Station Networks and Data Relay Systems. We contribute three key elements: (*i*) a detailed MCSS evaluation framework employing Monte Carlo simulations to assess space user links and distributions; (*ii*) a novel Space User Terminal (SUT) design optimized for MCSS, using different configurations and 5G New Radio Adaptive Coding and Modulation; (*iii*) extensive results demonstrating MCSS's substantial improvement over existing Ground Station Networks and Data Relay Systems, motivating its role in the upcoming 6G NTNs. The space terminal, incorporating a multi-system, multi-orbit, and software-defined architecture, can handle Terabit-scale daily data volumes and minute-scale latencies. It offers a compact, power-efficient solution for properly integrating LEO platforms as space internet nodes.**

***Index Terms*—6G, Non-Terrestrial Networks, Mega Constellations, Low-Earth Orbit Satellites**

I. Introduction

The onset of 6G wireless communication signifies a significant shift, broadening the scope of traditional terrestrial frameworks to include Non-Terrestrial Networks (NTNs) [1]. Encompassing Low Earth Orbit (LEO) satellites, High Altitude Platform Stations (HAPS), and Unmanned Aerial Vehicles (UAV), NTNs are set to be instrumental in the 6G ecosystem [2]. This expansion in scope is designed to overcome terrestrial network limitations, ensuring high-speed, ubiquitous connectivity, especially in remote and underserved areas [3]. Integrating NTNs with terrestrial networks promises to enhance global telecommunication, delivering broader coverage, increased data rates, and improved link reliability and disaster resilience.

NTNs are boosted by the "New Space" movement, a vital driver of the economy characterized by the burgeoning private sector engagement in space activities [4]. This era is marked by the deployment of an unprecedented number of cost-efficient LEO platforms (this term is used in this paper to encompass satellites, spacecrafts, platforms, etc., in Low Earth and Very Low Earth Orbits), serving a variety of functions, including Earth observation, remote sensing, science missions, positioning, navigation, and communications [5]–[8]. Particularly transformative is the emergence of mega-constellations, which consist of hundreds to thousands of satellites in LEO. Prominent examples like Starlink and OneWeb are revolutionizing satellite communications, significantly expanding the capabilities and reach of global connectivity networks [9].

While mega-constellations like Starlink and OneWeb are making strides in providing global terrestrial Internet connectivity, their integration into the NTN framework of 6G remains an open challenge for the community. The sporadic and time-bound nature of satellite communication links with ground nodes sets them apart from the persistent connectivity paradigm in 6G. Indeed, traditional communication methods between Earth and spacecraft are confined to short intervals when the satellite is visible to a ground station. Missing these brief communication windows results in delays from several minutes to hours before the next opportunity arises.

The principal workarounds to the sporadic connection problem are Ground Station Networks (GSNs) and Data Relay Systems (DRS), which leverage Geostationary (GEO) and Medium-Earth Orbit (MEO) satellites. However, these systems encounter notable challenges. GSNs are limited by their inherent constraints in installed capacity, complex operational scheduling, restricted visibility, and numerous logistical complexities. On the other hand, DRS systems face economic challenges due to the need for dedicated relay spacecraft in higher orbits, which restricts their broad applicability and diminishes their operational versatility. As a result, affordable, flexible, high-throughput, and low-latency communication solutions for nodes in LEO continue to be an elusive goal.

This paper addresses this limitation and integrates LEO platforms with NTNs by leveraging the Mega-Constellation Ser-

Authors' current address: Gabriel Maiolini Capez and Roberto Garello are with the Department of Electronics and Telecommunications, Politecnico di Torino, 10129 Turin, Italy (email: gabriel.maiolini@polito.it; roberto.garello@polito.it); Mauricio A. Cáceres and Stefan Frey are with Vyoma GmbH, 64295 Darmstadt, Germany (email: mauricio.caceres@vyoma.space; stefan.frey@vyoma.space); Roberto Armellin is with the Department of Mechanical Engineering, The University of Auckland, Auckland 1010, New Zealand (email: roberto.armellin@auckland.ac.nz); Chris P. Bridges is with Surrey Space Centre, University of Surrey, GU27XH Guildford, U.K. (email: c.p.bridges@surrey.ac.uk); Juan A. Fraire is with Inria, INSA Lyon, CITI, UR3720, 69621 Villeurbanne, France, and the Argentinian Research Council (CONICET), Córdoba, Argentina (juan.fraire@inria.fr). Corresponding author: Roberto Garello (email roberto.garello@polito.it).

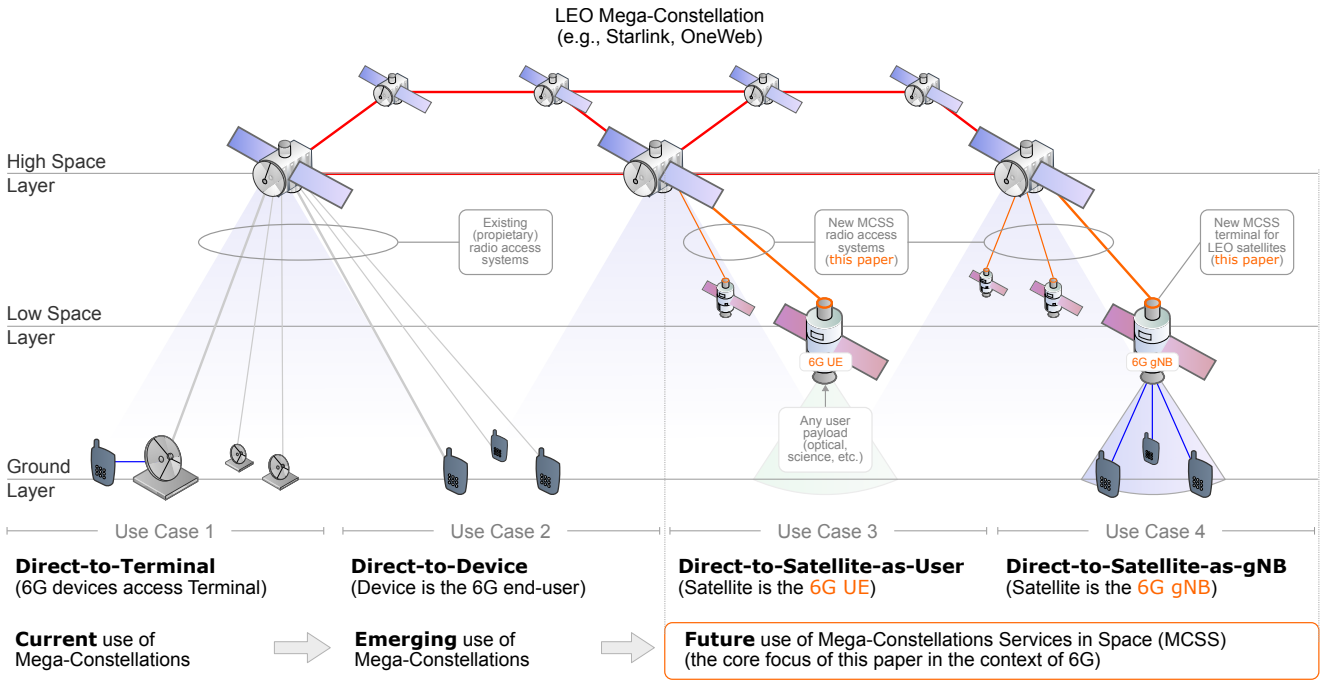

Fig. 1: Mega-Constellation Services in Space Paradigm in the context of 6G NTN Networks.

vices in Space (MCSS) paradigm. This approach, illustrated in Fig. 1, utilizes mega-constellations to extend the benefits in the terrestrial 6G domain to LEO spacecraft in lower orbits. The MCSS paradigm harnesses existing LEO mega-constellations' vast coverage and capacity for continuous, high-rate, and low-latency communication for LEO space assets acting as 6G User Equipments (UE) or 6G Next Generation NodeB (gNB). This paradigm shift enables LEO spacecraft to have uninterrupted internet access, starkly contrasting with the state-of-the-art GSNs and DRSs. The specific contributions of this paper are threefold.

1) *MCSS Evaluation Framework*: The first contribution is a comprehensive framework to assess LEO-NTN integration using MCSS. It applies Monte Carlo simulations to represent space user distributions and their orbital dynamics. This approach evaluates key coverage metrics like availability and latency, considering advanced link optimization techniques. Custom heuristics align the quality of service with terminal specifications and contemporary standards such as 5G New Radio (NR) for NTN [10].
2) *MCSS Space User Terminal Design*: The second contribution is a novel Space User Terminal (SUT) design tailored for LEO-NTN integration in MCSS. This design, embracing a multi-system, multi-orbit, and software-defined architecture, uses readily available components, ensuring versatility for various applications and compatibility with different mega-constellation providers. To obtain realistic results aligned with the most current trends, 5G New Radio (NR) Adaptive Coded Modulation, a strong candidate also for 6G, is considered for the space links.
3) *MCSS Evaluation Results*: The third contribution is a comprehensive set of results. The resulting analysis is the first to demonstrate that MCSS offers substantial improvements over existing GSNs and DRS. Through extensive evaluation of distinct SUT configurations, we showcase their capability to handle Terabit-scale daily data with end-to-end latencies in the order of seconds, low power consumption, and compact, lightweight designs.

This paper is organized into six key sections: Section II outlines MCSS and associated technologies. Section III details the MCSS model and its parameters. Section IV introduces our MCSS evaluation framework. Section V describes the design of the SUT. Section VI evaluates the SUT using our framework. Finally, Section VII concludes the paper.

II. Background

A. Non-Terrestrial Networks (NTNs)

The advent of 6th Generation (6G) wireless networks heralds a transformative era for NTNs, where integration with ground, air, and space-based systems is pivotal for achieving ubiquitous connectivity [2]. NTNs are set to play a significant role in 6G by providing seamless coverage and capacity augmentation, especially in regions where terrestrial infrastructure is limited or non-existent.

State-of-the-art developments in NTN 6G focus on an integrated approach that synergizes the capabilities of satellite systems, UAV, and terrestrial networks [1]. The convergence of these systems is designed to support a diverse array of applications, including Internet of Things (IoT) deployments, real-time control systems, and broadband services [3]. Advancements in inter-satellite links, beam-forming techniques,

and software-defined networking facilitate this integration, enhancing NTNs' flexibility and scalability.

In the context of integrated ground-air space systems, the role of satellites is undergoing a paradigm shift. Traditionally relegated to the status of backhaul or broadcast mediums, LEO satellites provide direct-to-terminal and direct-to-device services, as illustrated in Use Cases 1 and 2 in Fig. 1. Moreover, we claim that LEO satellites can be envisioned as active elements within the 6G network fabric. The architecture delineated in Fig. 1 outlines the prospective roles of satellites within this fabric:

1) *LEO Platform as UE*: In Use Case 3, satellites are considered as 6G User Equipment (UE), which can access services provided by mega-constellations via MCSS. This role enables satellites to act as aerial clients, requesting and utilizing network resources similar to terrestrial UEs within the spatial domain. Satellites as UEs are primarily assessed based on their ability to establish and maintain reliable links with the constellation, focusing on parameters such as link availability, latency, and data rates for individual satellite connections.
2) *LEO Platform as gNB*: In Use Case 4 envisions satellites as 6G Next Generation NodeBs (gNBs), where they receive services and provide connectivity to other UEs beneath their footprint. This role is instrumental in extending the reach of 6G networks, acting as aerial base stations that facilitate direct communication with ground, airborne, or other space-based assets. Satellites as gNBs are evaluated for their capability to manage multiple concurrent connections, for their capability to handle higher aggregate data traffic, and to provide consistent coverage over larger areas. This includes assessing the overall system throughput, the effectiveness of beam management, and the handover frequency.

As discussed in this paper, the MCSS radio access systems are integral to realizing these use cases. They offer a scalable and efficient framework for LEO mega-constellations to operate within the 6G ecosystem, either as UEs or gNBs, thereby enhancing the overall capacity and coverage of 6G networks. In the competitive landscape of MCSS, DRS and GSNs represent the performance and cost comparison baseline.

B. Data Relay Systems (DRS)

This section delves into the current state of DRS, exploring optical and Radio Frequency (RF) systems.

Substantial investments have been made in high-capacity transmission systems, such as the European Data Relay System (EDRS), due to their potential for high-speed data transfer. EDRS was initially deployed as a payload in Eutelsat 9B (EDRS-C) [11]. A second dedicated spacecraft in GEO (EDRS-C) [12] followed, which employed free space optical links to validate real-time relay to LEO satellites at 1.8 Gbit/s. However, these optical systems introduce complex operational and financial challenges. Current commercial MEO and LEO optical data relay constellations, such as Kepler's Aether Optical High-Data Rate Service [13], and other GEO optical relays primarily serving institutional users [14], face limitations in terms of coverage, scalability, and user capacity. Alternative technologies, such as hybrid RF/FSO systems, are also being researched and implemented. Hybrid RF/FSO systems aim to combine the strengths of both RF and FSO technologies, providing reliable communication links with higher data rates [15], [16]. However, these optical systems' premium cost and rigorous operational demands have led us to exclude them from our comparative analysis, focusing instead on more established and broadly applicable RF data relay solutions.

RF-based inter-satellite links offer several advantages over their optical counterparts. They facilitate continuous operation and provide a higher degree of autonomy. Furthermore, RF systems are not as heavily constrained by environmental conditions and do not require as rigorous temperature control and calibration, partly due to the use of wide-beam antennae (compared to narrow-beam laser systems). The core opportunities and challenges of inter-satellite links are discussed by Kodheli et al. in [4]. Additionally, emerging technologies like terahertz (THz) communications are being explored for their potential to offer ultra-high-speed data transfer [17], [18]. This makes RF systems a more practical choice for a broad range of applications, particularly in the current context of satellite communication infrastructure.

C. Ground Station Networks (GSN)

GSNs constitute a critical component in the global satellite communication infrastructure, offering a traditional yet essential means for data transmission between Earth and space assets [19]. GSNs typically consist of a network of terrestrial ground stations dispersed globally, ensuring varying degrees of coverage for satellite communications.

The primary strength of GSNs lies in their established technology and widespread deployment, providing reliable communication links for a range of satellites, including those in LEO, MEO, and GEO [20]. These networks facilitate satellite operations, including telemetry, tracking, control (TT&C), and payload data downlink. The Australasian Optical Ground Station Network (AOGSN) is a proposed network of 0.5 – 0.7m class optical telescopes across Australia and New Zealand that can also accommodate science and user data. A recent report from 2024 described the system as well as optimization alternatives in the context of cloud cover aspects [21].

However, due to the Earth's curvature, GSNs have limited visibility, restricting their access to satellites to specific time windows when satellites are within their line of sight. This limitation often delays communication, especially for LEO satellites that rapidly move in and out of a ground station's visibility. Moreover, the increasing number of satellites in orbit is leading to higher demand for ground station services, raising concerns about network congestion, availability, and the need for more complex scheduling mechanisms.

Recent advancements in GSNs focus on increasing automation [22], enhancing network capacity [23], and incorporating cloud-based data management solutions to better cope with the growing demands of satellite communication [24]. Additionally, integrating GSNs with NTNs and other emerging

technologies is being explored to expand communication capabilities and reduce latency in satellite data transmission [25].

D. Past work on Mega-Constellation Services in Space

The exploration of leveraging LEO mega-constellation links for communication began with H. Al-Hraishawi *et al.* in 2021 [26], where multi-layer space information networks were considered. This concept was further expanded upon by G. Maiolini Capez *et al.* in 2023 with a detailed characterization of the Mega-Constellation links for LEO Missions [27]. In the same year, H. Chougrani *et al.* contributed a feasibility study, emphasizing the significant potential of MCSS [28]. This growing interest in MCSS is also reflected in notable funding initiatives, such as the project under ESA's Open Space Innovation Platform, underscoring this innovative communication paradigm's increasing relevance and potential.

In the rapidly evolving landscape of MCSS, our paper offers the first detailed and comprehensive assessment framework for MCSS, complete with a novel terminal design and comprehensive performance evaluation. This work builds on the foundational studies conducted by Al-Hraishawi et al. and Maiolini Capez et al. and bridges the gap between theoretical feasibility and real-world application. The presented results allow us to fully understand the potential of MCSS within the 6G era.

III. System Model

A. Orbital Model

This subsection presents an overview of the core satellite orbital dynamics elements required for assessing and evaluating communication systems like MCSS. The position of a satellite at a specific moment in time, known as the *epoch*, is traditionally represented by six parameters, the Keplerian elements.

1) Orbit Size and Shape (a, e): The semi-major axis (a) and eccentricity (e) define the size and shape of an orbit. The semi-major axis represents the most extended radius in an elliptical orbit. Eccentricity, a dimensionless parameter, measures the orbit's deviation from a perfect circle. For circular orbits, the semi-major axis equals the orbit radius. The orbit radius is the sum of the altitude h and Earth's semi-major axis $r_a = 6378.137$ km, as specified in the WGS84 reference system [29].

The altitude h or an orbit defines if it is a LEO, MEO, or GEO orbit. LEO (Low Earth Orbit) is defined as the region of space around Earth at altitudes from about 160 kilometers (99 miles) to 2,000 kilometers (1,200 miles) above the planet's surface. MEO (Medium Earth Orbit), between LEO and Geostationary Orbit (GEO), typically ranges from 2,000 kilometers to 35,786 kilometers above the Earth's surface. GEO (Geostationary Orbit) is approximately 35,786 kilometers above the Earth's equator.

2) Orbit Orientation (α, Ω, ω): The orbit's orientation is defined by three angles: the inclination (α), the longitude of the ascending node (Ω), and the argument of perigee (ω). *i*) The inclination (α) is the angle between the orbit and a reference plane, usually the equator. *ii*) The longitude of the ascending node (Ω) indicates the orbit's horizontal orientation. *iii*) The argument of perigee (ω) determines the orbit's orientation within its plane.

3) Position in Orbit (ν): The true anomaly (ν) indicates the satellite's position in its orbit. For circular orbits, the argument of latitude u is used instead of the perigee's location.

We use orbital propagators to predict the spacecraft's future or retrospective positions and velocities.

4) Two-Body (2B) Propagator: The two-body propagator (2B) is a simple and efficient model based on gravitational forces between two bodies, typically a spacecraft and Earth [30]. It is ideal for short-term propagation but excludes effects like atmospheric drag and solar radiation pressure.

5) Simplified General Perturbations 4 (SGP4): SGP4 accounts for additional factors like gravitational perturbations and atmospheric drag, making it suitable for near-Earth satellites [31]. It uses Two-Line Elements (TLEs) from NORAD for satellite tracking, balancing accuracy and computational efficiency.

This study primarily uses the 2B model due to its computational efficiency and sufficient accuracy for both short—and long-term analyses. This model has been validated through comparative evaluations with SGP4 results.

B. Network Elements

The network elements considered in our system model comprise LEO users, LEO mega-constellations, and DRS systems in MEO and GEO.

1) LEO User Spacecraft: We refer to users as LEO satellites acting as a 6G UE or a 6G gNB element in the NTN ecosystem (see Fig. 1). Active LEO spacecraft predominantly occupy polar and near-circular orbits at altitudes ranging from 500-to-800 km, with inclinations varying between 45-to-90 degrees. Specific operational requirements of Earth Observation and communications satellites largely influence this distribution. Sensor coverage, satellite size, weight, power, and atmospheric drag are critical in determining these orbital choices. Consequently, the methodology proposed in this paper, which aims to evaluate the performance of LEO nodes within the MCSS paradigm, is especially relevant for these prevalent orbit types. This approach applies to satellites served by LEO mega-constellations and MEO/GEO relay constellations.

2) LEO Mega-Constellations: Mega-constellations are present in higher orbits than LEO user spacecraft and provide communication services in the MCSS paradigm (see Fig. 1). Our study centers on the OneWeb and Starlink Phase 1 mega-constellations, as outlined in Table I. These constellations, known as non-geostationary orbit (NGSO) systems, are primarily tailored for terrestrial usage. They feature highly directive antennas with robust side-lobe suppression, primarily facilitating connectivity for space users within the LEO environment. Starlink and OneWeb operate in overlapping frequency bands and share similar terminal configurations, hinting at the possibility of future terminals seamlessly switching between these networks. This paper also explores the combined service potential of a unified OneWeb+Starlink constellation setup.

TABLE I: OneWeb and Starlink Parameters

Name	Alt. [km]	Inc. [deg]	Planes	Sats/Plane	Total
OneWeb	1200	87.9	12	49	588
OneWeb	1200	55.0	8	16	128
Starlink	540	53.2	72	22	1584
Starlink	550	53	72	22	1584
Starlink	560	97.6	6	58	348
Starlink	560	97.6	4	43	172
Starlink	570	70.0	36	20	720

TABLE II: Communications Model Parameters

Parameter	Value
Satellite Selection	Closest
Channel Model	AWGN
Waveform	5G-NTN
MCS Spectral Efficiency	$\in$ [0.1, 5.8] bps/Hz
Power Amplifier	Linear or with Predistortion
Uplink Frequency	14.0 GHz
Downlink Frequency	12.7 GHz
Serv. Satellite Gain	36 dBi (LEO), 43 dBi (MEO, GEO)
Serv. Satellite TX Power	0 dBW (per user)
Serv. LEO Satellite G/T	8.7 dB/K
Serv. MEO/GEO Satellite G/T	18 dB/K
Serv. Satellite Pointing	Nadir
SUT. Pointing	Zenith
SUT. Min. El. Angle	25-degree
TX Insertion Losses (L_{TX})	1 dB
RX Insertion Losses (L_{RX})	1 dB
Implementation Loss (L_{impl})	1 dB
Polarisation Loss (L_{pol})	0.25 dB
Pointing Loss (L_{point})	3 dB
Side-lobe level	See Antenna
Synchronisation	Genied-aided (perfect sync.)
Link Margin M	3 dB
Protocol Overhead (OH)	20%
Safety Margin	20%

3) MEO and GEO DRS: Our study also delves into the feasibility of integrating existing RF data relay systems in MEO and GEO with the MCSS framework. This integration is increasingly plausible, evidenced by recent industry movements such as the acquisitions and integrations of Ku-band satellite operators (e.g., Eutelsat, Intelsat) and the development of multi-orbit terrestrial terminals. In particular, we focus on SES's MEO O3b mPOWER (in MEO) [32] and Eutelsat's Ku-band Satellites (in GEO) [33], both frequently cited in industry and academic circles as viable data relay solutions [13], [34]–[36]. To ensure representative analysis, the orbital configurations of these MEO and GEO satellites are derived directly from CelesTrak data [37]. These systems, with their distinct orbital characteristics and capacities, could significantly augment the capabilities of MCSS, providing enhanced coverage, capacity, and resilience in space-based communications networks.

C. Communications Model

This subsection presents the core communication models used in our evaluation framework and terminal design. The discussed parameters are summarized in Table II.

1) Sources: FCC and ITU: To create a realistic communication scenario, our communication model utilizes technical information from FCC filings related to Earth Stations (terminals, gateways) and Space Stations (satellites) of specific satellite operators [38], [39]. Our analysis considers the specifications detailed in the FCC filings for the Phase 1 deployments of Starlink and OneWeb. Starlink's mega-constellation primarily comprises 4408 satellites across various orbital planes, as specified in their FCC filings approved in April 2021. OneWeb's system in Phase 1, initiated in April 2016, was initially planned to consist of 720 non-geostationary satellites at a 1200 km altitude. Still, it was later modified to 716 satellites with some orbital plane adjustments. This approach ensures our model aligns with operational satellite constellations, offering robustness and accuracy in representing deployed systems and their coverage. Furthermore, our model considers the guidelines set by the International Telecommunication Union (ITU) [40], specific to non-geostationary orbit satellites functioning in the fixed-satellite service at frequencies below 30 GHz. Finally, we consider the link budget analysis outlined in [41].

2) G/T and EIRP: For the G/T and EIRP considerations, we use the minimum G/T value of approximately 8.7 dB/K and the maximum Effective Isotropic Radiated Power (EIRP) from the Starlink and OneWeb mega-constellations FCC filings [38], [39]. In the case of MEO and GEO satellites, we consider a typical G/T range of 13-to-20 dB/K for Ka-band [42]–[44], equivalent to a Ku-band G/T of 7-to-15 dB/K for similar antenna apertures [10], [45], [46]. With this in mind, we postulate a G/T value of 18 dB/K and an antenna gain (G) of 43 dBi. This range is based on Eutelsat's technical specifications and relevant literature, and it is vital for evaluating communication link performance across different satellite services.

3) Beams: Mega-constellations employ thousands of narrow beams to optimize performance in targeted areas. While this approach aids performance optimization, it introduces interference management, resource allocation, and complexities of beam-switching logistics. It is particularly challenging to accommodate the high mobility of space users in LEO, who move quickly across beams due to their high velocity. Additionally, the high mobility of space users poses challenges in maintaining consistent coverage and capacity. Frequent beam crossings by space users necessitate adept beam management through steering or switching to ensure continuous, high-quality communication for a dynamic group of space users. This is especially true for Very-High Throughout MEO/GEO services considered in this paper.

4) Antenna: We adopt an analytical approximation of LEO mega-constellations radiation patterns per ITU guidelines to simplify the coverage analysis. The equation from [40] defining the gain in dBi is as follows:

$$G(\Psi) = \begin{cases} G_m - 3(\Psi/\Psi_b)^{\alpha}, & \text{if } 0 < \Psi < a\Psi_b \\ G_m + L_N - 20\log(z), & \text{if } a\Psi_b \leq \Psi < 0.5b\Psi_b \\ G_m + L_N, & \text{if } 0.5\Psi_b \leq \Psi < b\Psi_b \\ X - 25\log(\Psi), & \text{if } b\Psi_b \leq \Psi < Y \\ L_F, & \text{if } Y \leq \Psi \leq 90 \\ L_B, & \text{if } 90 < \Psi \leq 180. \end{cases} \quad (1)$$

Here, Ψ is the off-axis angle; $X = G_m + L_N + 25log(b\Psi_b)$; $Y = b\Psi_b 10^{0.04(G_m+L_N-L_F)}$; Ψ_b is one half the 3-dB beamwidth in the plane of interest (3-dB below G_m); $G(\Psi)$ is

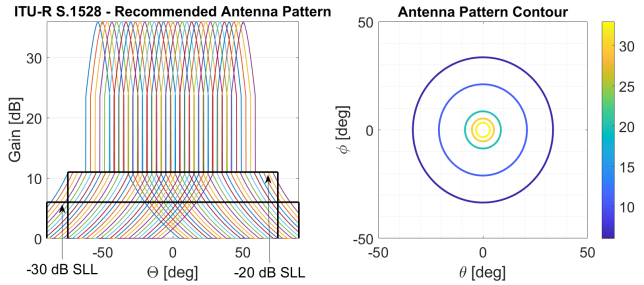

Fig. 2: Approximate Starlink Radiation Pattern

the gain at the angle Ψ from the main beam direction; $G_m = 36\ dBi$ is maximum gain in the main lobe; $L_N = -25\ dB$ is the near-in side-lobe level relative to the peak gain required by design; $L_F = 0\ dBi$ is the 0-dBi far-out side-lobe level; $L_B = 0\ dBi$ is the back-lobe level; $z = 1$ is the major/minor axis for the radiated beam; and $a = 2.56$, $b = 6.32$, and $\alpha = 1.5$ are constants provided in the recommendation. The results of this approximation for Starlink can be seen in Fig. 2. Furthermore, we adopt a minimum elevation angle of 25 degrees for the user antenna, a practical value for both passive and active antenna types. To describe GEO and MEO coverage, we consider that all beams fall within a 10.5-degree and 26-degree half-cone, respectively. This ensures that no signal radiates beyond the Earth's edges.

5) Channel Model:

a) AWGN: Our analysis framework characterizes the communication channel as an Additive White Gaussian Noise (AWGN) line-of-sight channel, assuming flat fading conditions and excluding multi-path effects and sun noise interference.

b) Doppler: Our previous study in [27] thoroughly analyzed the Doppler effect within the MCSS framework, focusing on the Doppler offset and rate implications for SUTs. We determined that in the Ku-band, SUTs experience a maximum Doppler offset of up to 550 kHz. The Doppler rates observed range from below 2 kHz/s at elevation angles lower than 70 degrees to approximately 20 kHz/s when the satellite is directly overhead (at the Zenith). Considering these dynamics, our analysis presupposed that the receiver architecture within SUTs can inherently compensate for such Doppler offsets. This compensation may be inherent within the receiver's design or facilitated through Doppler pre-compensation techniques. These techniques involve the satellite and the SUT applying adjustments based on constellation ephemerides and precise position, navigation, and timing information. Further discussed in the SUT design section, this approach is critical for ensuring accurate signal processing and maintaining the integrity of communications despite the rapid relative motion between satellites and SUTs.

6) Adaptive Modulation and Coding: Mega-constellations like Starlink and OneWeb employ Orthogonal Frequency-Division Multiplexing (OFDM)-based waveforms, a technique also foundational to 5G New Radio (NR), and a candidate for future waveforms in 6G [47]. Therefore, we focus on the 5 G waveform to illustrate the potential for integration with terrestrial and NTNs. This approach allows us to explore how MCSS can leverage standard 5G-NR bandwidths and adapt to conventional 5G parameters, such as 5, 10, and 20 MHz bandwidths.

According to 5G-NR, we model Adaptive Code and Modulation (ACM). To implement this, we have devised a comprehensive look-up table encompassing a broad spectrum of Modulation and Coding Schemes (MCSs), ranging from basic Binary Phase-Shift Keying (BPSK) to more complex schemes like 256-QAM/APSK. From this table, we select the MCS that offers the highest Spectral Efficiency (SE) for each epoch or predefined time interval. This selection is aimed at maximizing the net user data rate, $R^{ti}_{SUT,l} = (1 - OH) * R_s * SE\ [bps]$. Here, R_s represents the symbol rate, and OH denotes the protocol overhead. By dynamically adjusting the MCS in response to changing channel conditions, we can optimize the data throughput, ensuring the most efficient use of the available spectrum and maintaining robust link performance.

Based on these communication parameters and the range from the orbital dynamics, we calculate the received Es/N_o (Energy per Symbol to Noise Power Spectral Density) ratio. This is compared against the threshold required for a chosen MCS to ensure the link's viability and adherence to performance standards. To this end, we leverage the following equation:

$$\left.\frac{E_s}{N_o}\right|_{sim} = EIRP(\theta,\phi) - PL + \frac{G(\theta,\phi)}{T} - 10\log_{10}(kB) - L_{impl.} - L_{other} - M \geq \left.\frac{E_s}{N_o}\right|_{ref} \text{[dB]}. \tag{2}$$

Here, $EIRP(\theta,\phi)$ is the transmitter's EIRP; $G(\theta,\phi)/T$ is the receiver's figure of merit; k is the Boltzmann constant; B is the bandwidth; L_{impl} is the implementation loss; PL is the propagation loss; L_{other} represents all additional impairments and losses.

7) Error Recovery: As mentioned, our study's E_s/N_o thresholds are based on classical link-level simulations. These thresholds are set to ensure operation in a quasi-error-free regime, targeting a Block Error Rate (BLER) of less than $1E-5$, without relying on (hybrid) Automatic Repeat Request (ARQ) mechanisms. It is assumed that digital pre-distortion techniques or suitable back-off strategies are employed to maintain the signal's integrity within these parameters.

8) Margins: Our design incorporates a comprehensive margin consideration for potential impairments and operational challenges. Specifically, we include:

- A 3-dB margin for potential interference and to counteract synchronization issues related to carrier, timing, phase, and frame.
- An implementation loss margin of 1 dB.
- Insertion losses at the transmitter and receiver are accounted for with an additional 1 dB per device.
- Polarization losses, particularly for circular polarization, are estimated at 0.25 dB.
- Pointing losses are factored in at 3 dB, anticipating minor misalignments in antenna pointing and edge-of-coverage service (user within satellite's half-power beamwidth).

Furthermore, to address other possible challenges, such as excessive interference, sun noise, or issues stemming from

radio resource management (scheduling constraints, service channel collisions, and handovers), we apply a 20% reduction to the calculated capacity. Additionally, we consider a 20% protocol overhead in our calculations.

9) Concurrent Users: With frequency division, concurrent users can access user-to-gateway channels, following OneWeb's single-carrier frequency division multiple access (SC-FDMA) model in FCC filings.

IV. Evaluation Framework

In this section, we leverage the presented system model to introduce an evaluation framework to assess the expected performance of the Mega-Constellation Services in Space (MCSS) paradigm, integrating LEO satellites with serving Mega-Constellations in the context of NTNs.

The proposed solution incorporates several new ideas that enhance its robustness and relevance. Firstly, we developed a comprehensive Monte Carlo simulation framework that models a wide range of scenarios and user distributions, providing a detailed analysis of link availability, latency, and data rates across different orbital configurations. Our evaluation includes a detailed orbital dynamics analysis, considering the impact of varying altitudes and inclinations on system performance. We also explored the potential of satellite-to-satellite links, assessing their impact on enhancing communication reliability and data rates. Furthermore, the evaluation includes an analysis of integrating multiple satellite systems, such as OneWeb, Starlink, and O3B, to highlight the benefits and challenges of such integration in improving overall system performance.

The evaluation framework provides coverage and link analysis insights for LEO nodes accessing serving mega-constellations. With this in mind, LEO can stand equally for LEO Platform as UE and LEO Platform as gNB. In other words, from the evaluation framework perspective, there is no difference between satellites such as UE and satellites such as gNB.

The following subsections detail the Monte Carlo Approach and a two-stage evaluation pipeline.

A. Monte Carlo Approach

To address the computational challenges presented by mega-constellations vast service areas and their radio payloads' dynamic nature, we implemented a Monte Carlo simulation method [48]. We modeled 1000 LEO user spacecraft uniformly distributed across the principal orbital planes. To increase precision within the most constrained geometrical zones, we strategically placed an additional 100 users near the peak altitudes of each constellation ([470 570] km, [1100 1200] km). We refined our approach through iterative runs and utilized the outcomes for a sensitivity analysis to fine-tune our capacity estimates. It was determined that starting with 5000 SUTs yields a robust estimate of system capacity with a 60-second timestep across a 24-hour window. For latency metrics, we ran simulations with 19650 LEO users from the OneWeb constellation at one-second intervals over 128 minutes, guaranteeing the capture of a complete orbital period for every user's trajectory.

B. Two-Stage MCSS Evaluation Algorithm

The evaluation algorithm is presented in Fig. 3 and discussed below.

① *Scenario Configuration:* Inputs to the algorithm consist of a pre-defined scenario encapsulating various elements, including the simulation timeframe, resolution, and Monte Carlo MC iterations; details of the satellite constellation such as configuration type (e.g., Walker or Flower) and elements (from Two-Line Element sets, TLEs); space user orbital parameters derived from TLEs or distributed across designated (altitude, inclination) bins; RF payload specifications of the constellation including waveform, antenna beams, minimum elevation angle, and frequency resources; SUT configurations; and predefined user policies dictating satellite selection and link or coverage constraints.

② *Space Segment Initialization:* After scenario input, the algorithm initiates by defining the positions of all constellation satellites using the following state vector, setting the stage for propagation and interaction analysis within the MCSS framework:

$$s_{SAT}^{t_0} = \left\{ \left(r_{Sat,1}^{t_0}, v_{Sat,1}^{t_0} \right), ..., \left(r_{Sat,N_{Sat}}^{t_0}, v_{Sat,N_{Sat}}^{t_0} \right) \right\} \tag{3}$$

Where $r_{Sat,m}^{t_0}$ and $v_{Sat,m}^{t_0}$ are the initial position and velocity of the constellation satellite m in Cartesian coordinates (x, y, z) in the True Equator Mean Equinox (TEME) frame [49]. This space vector is determined from TLEs or by an ad-hoc constellation generator. To accurately model the orientation of satellite antennas, each satellite within the constellation is aligned with a Radial, Transverse, Normal (RTN) frame. This enables the precise alignment of the antenna beams concerning the satellite's position. We operate assuming that each satellite is equipped with a Nadir-pointing body-mounted antenna, which aligns with the Z-axis of the RTN frame. The antenna beams are sequentially numbered from 1 to N_{Beams} for effective beam representation. Each beam is then assigned a set of off-Nadir angles, denoted by Θ_{Sat}, and guides the orientation of the beams concerning the Nadir direction. Employing the antenna radiation pattern masks, we can then ascertain the relevant antenna gain for each beam, ensuring an accurate simulation of the satellite's communication footprint.

③ *Space User Segment Initialization:* With the space segment established, the Monte Carlo iteration counter is set ($Cntr_{MC} = 1$), and the space user segment is created by sampling orbital parameters from a defined distribution of Keplerian elements, as specified in the scenario. A new set of space user elements is generated for each MC iteration, ensuring a comprehensive examination of the operational environment. Each SUT is allocated a Radial, Traverse, Normal (RTN) frame for orientation. It is assumed that every SUT is equipped with a Zenith-pointing body-mounted antenna aligned with the negative Z-axis of the RTN frame. Instead of delineating specific antenna beams, a satellite's visibility is determined solely based on the off-Zenith angle, providing terminal designers with the flexibility to optimize antenna design within the bounds of a viable minimum elevation angle. This approach simplifies the design process, although a

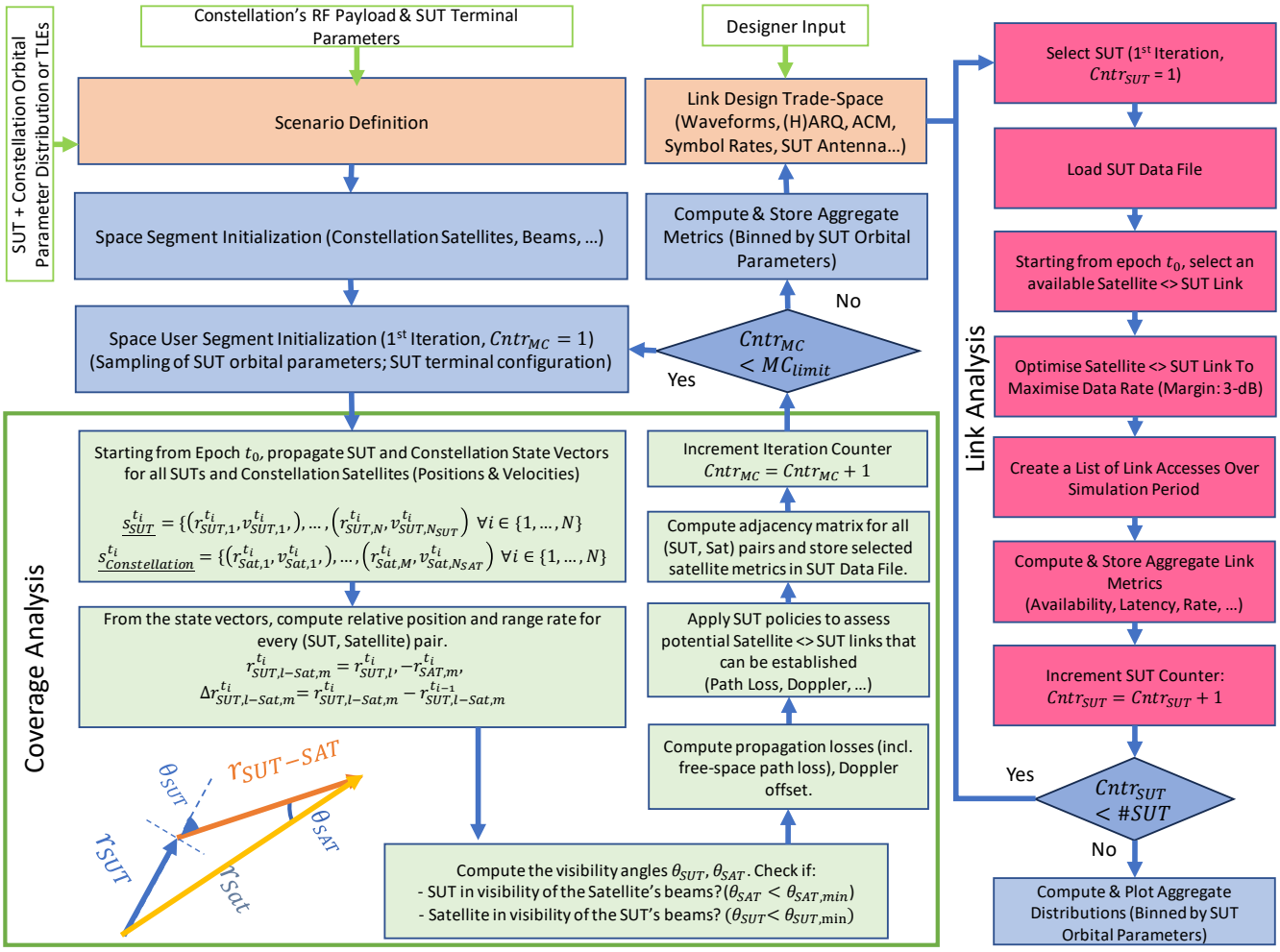

Fig. 3: MCSS Evaluation Algorithm

specific radiation pattern mask can be applied if detailed beam characterization is necessary.

④ *Coverage Analysis:* Over time, the algorithm propagates satellite and SUT positions in each Monte Carlo iteration. It calculates the relative positions and velocities for each (SUT, satellite) pair, allowing for the estimation of relative range, range rate, and the off-Nadir/off-Zenith angles (Θ_{SAT}/Θ_{SUT}). The next step is to determine the illumination status of a SUT by a satellite's beam. This is done by comparing Θ_{SAT} and Θ_{SUT} with the respective antenna radiation patterns and the minimum elevation angle required for the SUT. A positive match indicates that the line-of-sight condition for the channel is met. Subsequently, the algorithm calculates the associated propagation losses and the Doppler offset. Based on these metrics, the algorithm enforces user policies such as path loss and Doppler constraints to filter suitable satellite links. The outcome of these policies informs the creation of an adjacency matrix that maps potential satellite-SUT connections. Coverage metrics are then compiled into a data file for each SUT, encapsulating the accessible links and facilitating further analysis.

⑤ *Coverage Metric Computation and Categorization:* After the coverage analysis iterations, the resulting data is organized into bins according to the users' orbital parameters. The categorized information visually highlights key coverage metrics, such as satellite availability, access duration, and path loss. This bifurcation of coverage and link analysis simplifies the optimization process, enabling system designers to fine-tune both system-level (e.g., constellation layout, user dynamics) and link-level (e.g., waveform selection, data rate) parameters with greater ease. The dual-stage nature of the algorithm also facilitates the parallel execution of multiple link-level analyses or higher-tier evaluations.

⑥ *Link Design Trade-Space:* Designers determine the specific terminal design parameters by leveraging the insights gained from coverage metric visualizations or as part of the initial scenario configuration. These parameters include waveform, bandwidth, antenna characteristics, re-transmission mechanisms, pointing accuracy, channel model, ACM, and the array of supported MCS. These selections form the foundation of the subsequent link analysis, where the interaction between the terminal and the network is scrutinized to assess terminal performance and identify optimal design trade-offs.

⑦ *Link Analysis:* This stage of the algorithm operates within the trade-space parameters established previously. It processes the coverage data for each SUT (④), initiating from

the first epoch t_0. The algorithm prioritizes the selection of a Satellite-SUT link that aligns with predefined user policies and optimizes the data rate, taking advantage of ACM when available. Without ACM, it opts for the best rate that ensures the highest availability. For the purposes outlined in this paper, we have chosen to fix the user bandwidth and focus on optimizing the Modulation and Coding Scheme (MCS) selection. Upon reaching the end of the designated simulation period, the algorithm aggregates the data, compiling a comprehensive list of link accesses and their corresponding metrics throughout the simulation. These metrics include daily capacity and percentile distributions for availability, latency, and rate.

⑨ *Finalization:* The algorithm's final step involves categorizing the link data according to user orbital parameters. This data is then visualized graphically, providing an intuitive understanding of the link performance across different orbital profiles. This visualization aids in the final assessment and validation of the MCSS framework's effectiveness compared to its alternatives.

V. Terminal Design

The design of the SUT is critical to achieving the seamless integration of LEO platforms with NTNs in the emerging 6G communication landscape. Our user terminal design introduces several innovative features that address the unique challenges of this integration.

The novelty of our user terminal design is anchored in its multi-system, multi-orbit compatibility, enabling seamless operation across different mega-constellation systems and orbital regimes. This design incorporates 5G New Radio (NR) Adaptive Coding and Modulation (ACM), which dynamically adjusts to varying channel conditions, optimizing data throughput and link reliability. The terminal's compact and power-efficient architecture also supports Terabit-scale daily data volumes and minute-scale latencies, making it a versatile and robust solution for integrating LEO platforms into the 6G ecosystem. The software-defined modem enhances the terminal's adaptability, providing frequency agility and advanced signal processing capabilities.

Fig. 4 presents our versatile MCSS Space User Terminal (SUT) architecture, compatible with multiple systems and orbital regimes. It comprises four main components:

1) Constellation Scheduler: Orchestrates communication sessions with constellation satellites, considering availability and constraints.
2) Antenna Subsystem: Includes antenna, antenna controller, and optionally, reconfigurable antennas for aligning with various constellation satellites.
3) Ku-band RF Front-end: Contains up and down conversion stages, a high-power amplifier for transmission, and a low-noise amplifier for reception in the Ku-band.
4) Multi-Channel Software-Defined Modem: Links the RF front-end with spacecraft subsystems like GNSS, AOCS, and OBC for integrated navigation, control, and data handling.

Table III outlines four SUT configurations, each suited for different mission requirements and budgets:

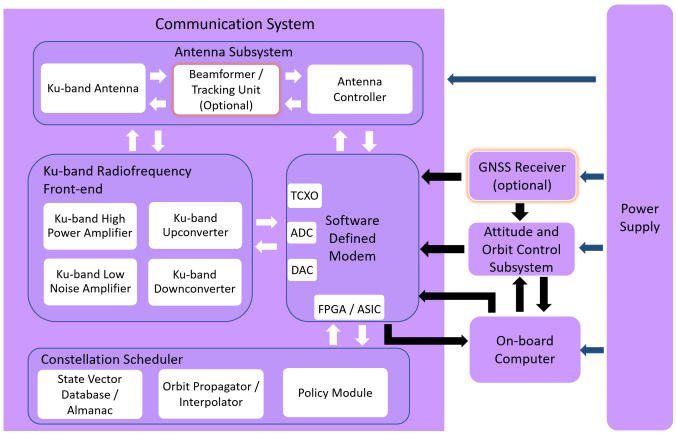

Fig. 4: Space User Terminal (SUT) architecture.

- High-End (HE/HE+): Features beam-steering and an advanced modem supporting up to 20 MHz bandwidth, with 10 cm and 30 cm antenna apertures for HE and HE+, respectively.
- Common Case (CC): A standard model with Software Defined Radios, 8-dBi gain antennas, and 10 W transmitted power.
- Low-End (LE): Budget-friendly with hemispherical antennas and a 2.5 W transmit power cap.

The SUT's modem includes a Temperature-Compensated Crystal Oscillator (TCXO), DAC/ADC converters, and an FPGA or ASIC, offering frequency agility and dynamic power control. It interfaces with the spacecraft's onboard computer and AOCS for navigation, timing, and beamforming.

The Constellation Scheduler, crucial for effective satellite communication, encompasses a State Vector Database, Orbit Propagator, Signal Acquisition and Synchronization unit, Beam-Steering Management, and a Policy Module for managing satellite links.

The antenna subsystem, essential for service quality, varies per service requirements:

1) High-Throughput Services: Requires high-gain antennas with active steering/forming and a wide tracking beam.
2) Common Case: Features circular polarization, 8-dBi uplink gain, and 10 W uplink power.
3) Antenna Specifications: Should have at least 3.5% uplink and 17% downlink fractional bandwidth, with a reflection coefficient below -10 dB and an axial ratio below 6 dB.

A wide-beam patch antenna is a cost-effective solution, meeting performance criteria while minimizing expense and resource demands.

The Electrical Power Subsystem (EPS) influences operational dynamics if the transmitter is to be operated at a 100% duty cycle:

1) Continuous Power Consumption: Poses challenges for spacecraft relying on photovoltaic cells.
2) Battery and Solar Array Requirements: Larger batteries and solar arrays are needed for continuous operation.
3) Mission Design Considerations: Requires reevaluation of EPS design and operation strategies.

Configuration	Low-End (LE)	Common Case (CC)	High-end (HE)	High-end+ (HE+)
Output Power [dBW]	+4	+10	+9	+9
TX Bandwidth [MHz]	10	20	20	20
RX Bandwidth [MHz]	5	5	5	5
G/T [dB/K]	-21.7	-16.7	-4.7	+5.3
Antenna Gain [dBi]	+3	+8	+20	+30
Antenna	Passive	Passive	Active	Active
# Beams	1	1	≥ 3	≥ 3
Input Power [W]	<25	<45	45-100	45-100
Weight [kg]	< 1	< 1.5	≥ 2	≥ 2
Form Factor	<1U	< 1U	2U	3U
Handover	Digital	Digital	Hybrid (Beam-Steering + Digital)	Hybrid (Beam-Steering + Digital)
Complexity	Lowest	Low	High	High
Role in MCSS	LEO as UE	LEO as UE or gNB	LEO as UE or gNB	LEO as gNB

TABLE III: Space User Terminal Configurations.

4) Challenges for Smaller Platforms: Accommodating a powerful EPS in CubeSats and NanoSats is challenging.
5) Thermal Management and Structural Considerations: An always-on terminal requires careful thermal regulation and robust deployment mechanisms for larger solar arrays.
6) AOCS Requirements: The terminal must maintain an attitude that ensures antenna alignment towards the zenith.

The SUT is meticulously tailored to manage the high channel dynamics characteristic of satellite communications. Central to this design is implementing guard bands strategically set at twice the maximum Doppler offset (about 1 MHz). This crucial feature mitigates potential interference and averts frequency collisions, thereby upholding the integrity and reliability of communications. To this end, the SUT design integrates Doppler pre-compensation mechanisms. This development is particularly noteworthy in the context of LEO mega-constellations and their integration into the 6G NTN context.

Table III details the hosting impacts for each terminal configuration, allowing adaptation to various satellite platforms.

VI. Results Analysis

This section evaluates the performance of various SUT configurations within the MCSS framework, highlighting its adaptability to diverse user needs. We showcase MCSS's capability to connect space users with multiple constellation satellites, significantly influencing SUT architecture. We also explore the potential for providing low-latency broadband to space users, significantly surpassing data relay systems and ground station networks. The results discussed below apply to both NTN roles of the satellites equipped with the SUT: LEO as UE and LEO as gNB.

A. SUT Performance Analysis

The main performance results are presented in Fig. 5 (Common Case availability and capacity), Fig. 6 (High-End handovers), and Fig. 7 (Common Case latency), Fig. 8 (High-End capacity), Fig. 9 (High-End+ capacity). We discuss the different aspects below.

1) Daily Capacity Analysis for Different SUT Configurations: For uplink (UL) capacity, the common-case (CC) configuration reaches up to 2.5 Tbit/day with a 20 MHz bandwidth. High-end (HE) configurations can achieve more than 5 Tbit/day for uplink. These results are extremely good for transmitting payload data from a high-performance UE or a gNB operating in an LEO satellite. Although not reported for brevity, the low-end (LE) configuration still delivers up to 500 Gbit/day using a 10 MHz bandwidth and less than 2.5 W power, demonstrating MCSS's efficiency in data transfer even with low-power setups suitable for 6G UE. Regarding downlink (DL) capacity, CC and HE configurations offer substantial throughout, crucial for telecommand operations, with several hundred Gbit/day.

2) Influence of Orbital Altitudes on SUT Capacity: As expected, user orbital altitudes markedly influence the capacity of SUTs. Understanding the correlation between user orbits and daily capacity is vital for optimizing MCSS deployment for varying orbital profiles. In the CC configuration, lower altitude users (350-550 km range) consistently achieve more than 2 Tbit/day in uplink and at least 500 Gbit/day in downlink. However, higher altitudes lead to performance degradation, primarily due to reduced link availability from the limited line of sight with constellation satellites. This decline is notable above 900 km, where link availability can fall to 10-20%, beyond the compensatory range of rate adjustments in CC configurations. In HE configurations, performance is better but also decreases with altitude. Yet, beyond Starlink's altitude, ACM helps counteract this by increasing data rates to compensate for lower path losses and availability. This scenario illustrates a trade-off between constellation altitude, link availability, data capacity, and latency, particularly for users at 550-750 km altitudes. Here, a slight decrease in availability is balanced by higher data capacity but at the cost of increased latency. An alternative approach for high-altitude users could be using the side lobes of constellation satellites, though this introduces challenges in managing interference between beams. Proper exploitation of sidelobes is appealing for future research in the context of MCSS.

3) Impact of User Orbits on Daily Latency: Besides capacity, the orbital parameters of SUTs significantly impact average data latency, which is the duration of disconnection from the mega-constellation. Low altitude SUTs or those near critical

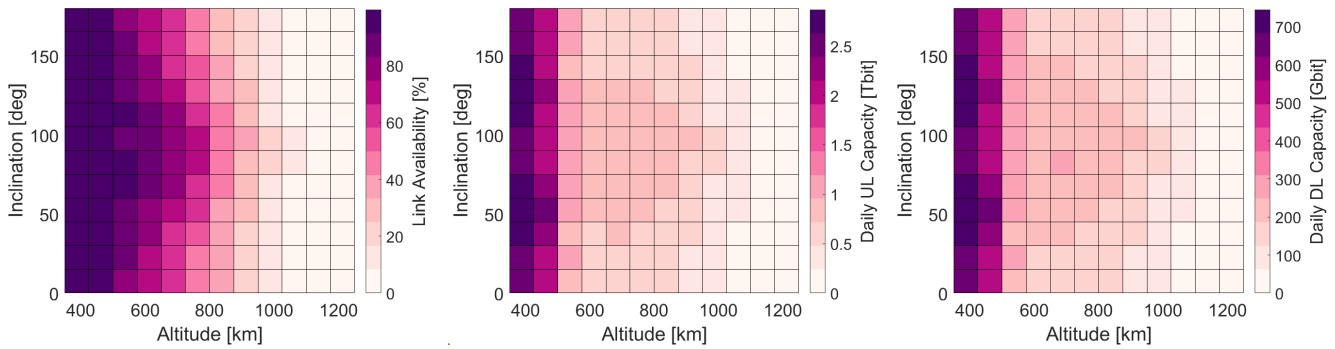

Fig. 5: MCSS Performance Envelope for CC configuration using OneWeb (OW) + Starlink (SL). Left-to-right: Availability, UL (Payload, Telemetry) Capacity, and DL (Telecommand) Capacity.

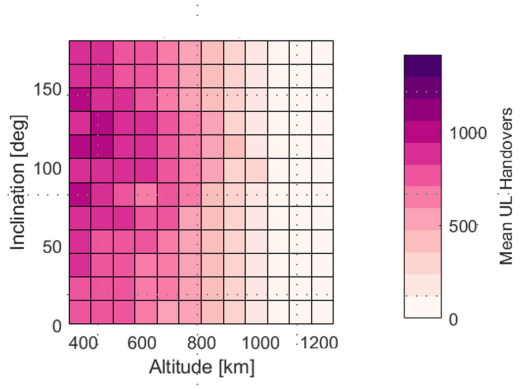

Fig. 6: MCSS uplink daily handover metrics for CC configuration and OneWeb constellation.

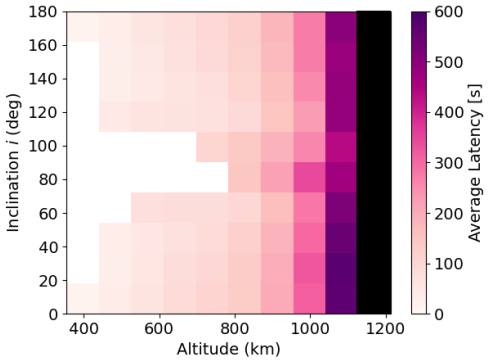

Fig. 7: MCSS Latency for CC configuration and OneWeb constellation. The Z-axis is limited to 600 seconds (10 minutes). Black indicates no coverage/latency. White corresponds to nominal mega-constellation latency (about 50 ms).

inclinations provide the best latencies: they can maintain nominal Mega-Constellation latencies (approximately 50 ms) with brief disconnections, as shown in Fig. 7. These results are extremely important for integrating LEO satellites as UE or gNB of the 6G network because, as discussed in Section II-C, the latencies obtainable from a state-of-the-art Ground Station Network are 20 minutes. This applies to typical Earth-observation and remote sensing LEO satellites, as illustrated in use cases 3 and 4 in Fig. 1. We observe that retrograde orbits around these inclinations have marginally better latency due to faster satellite motion, which reduces coverage gaps. However, as the SUT altitude increases, both coverage and latency worsen. At altitudes above 1000 km, where coverage drops to 10% or less, latencies akin to GSN (greater than 10 minutes) are expected. UE with sporadic connectivity can be considered at such altitudes, but a gNB above 1000 km is unlikely to operate correctly with MCSS.

4) Impact of Multi-Channel Availability on SUT Efficiency: SUTs below 750 km altitude experience higher multi-channel availability (i.e., multiple satellites in the mega-constellation are reachable), particularly at critical orbital inclinations. Typically, 2 to 4 satellites are in the line of sight with a 25-degree minimum elevation angle and 1 to 4 satellites with a 40-degree angle. However, visibility reduces to fewer than two satellites beyond 55-degree inclinations due to satellite positioning limitations. The evaluation framework reports this decrease affects coverage but isn't shown in this study due to space limitations. In a common-case (CC) SUT configuration, access to four channels is critical to maximize capacity and ensure seamless satellite handover. This is crucial for both LEO with UE and gNB roles.

5) Impact of Handover Count in Serving Constellations: Fig. 6 illustrates the average daily handover count for the CC configuration (OneWeb constellation). We assume a simple HO criteria: the closest satellite is chosen as the serving satellite. As a result, handover frequency increases at lower altitudes due to the accessibility of multiple serving satellites and the higher orbital speed of the SUT.

6) Maximum Concurrent Space Users: To estimate the maximum number of simultaneous SUTs the MCSS can support, we use equation (4). Here, BW_{Sat} (500 MHz) is the uplink bandwidth in the Ku-band, the primary constraint for space users. The guard band allocation is $BW_{Guard\ Band}$ (1.1 MHz). The number of satellites (N_{Sat}), beams per satellite ($N_{Beams/Sat}$), and polarisation per beam ($N_{Polariz/Beam}$) depend on the specific constellation, and k is the frequency re-use factor. Taking OneWeb as an example, with 16 beams per satellite, a low-frequency re-use factor (k = 2), and 716

$$N_{Users} = \left\lfloor \frac{BW_{Sat} - N_{Users/Sat} \times BW_{Guard\ Band}}{BW_{User}} \right\rfloor \times \frac{1}{k} \times N_{Sat} \times N_{Beams/Sat} \times N_{Polariz/Beam} \quad (4)$$

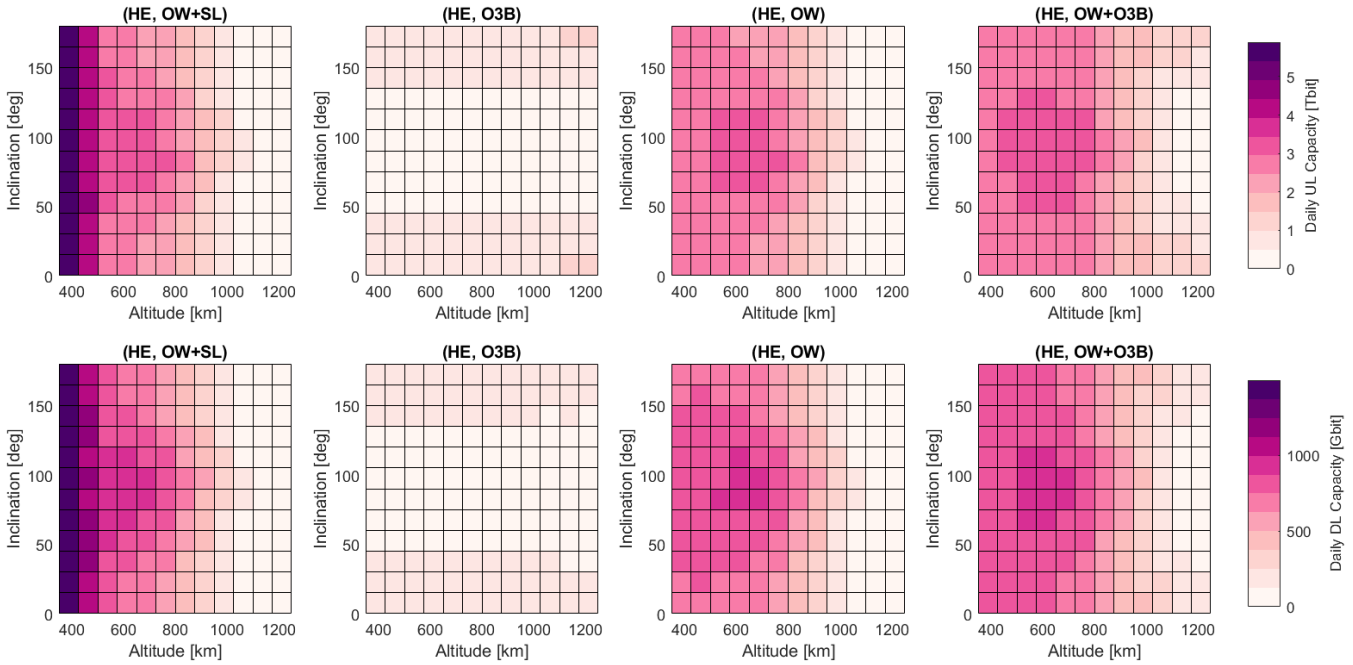

Fig. 8: MCSS capacity for HE configuration using multiple constellations. Left-to-right: OneWeb and Starlink (OW+SL), O3B mPOWER (O3B), OneWeb (OW), and OneWeb and O3B mPOWER (OW+O3B). Top: UL. Bottom: DL (Eutelsat not represented because path losses are too high to close the link).

satellites, the constellation can support thousands of SUTs. However, satellite capacity, predominantly tailored for terrestrial users, is a limiting factor. Terrestrial demands typically utilize 20-30% of network resources, with satellites often reaching total capacity during peak times [50]. Considering mega-constellations are optimized for ground users, space users should expect limited access to a constellation's capacity. With dynamic traffic patterns and congestion management requirements, up to 90% of capacity may be reserved for ground users. Given these conditions, the system could support approximately 4,000 SUTs in the High-End (HE) configuration to 100,000 SUTs in the Low-End (LE) configuration. This capacity range is well-suited to current space mission scales, indicating MCSS's aptness for the existing space user community's needs.

B. Multi-System Integration

Finally, this section discusses how integrating MCSS with Data Relay Systems can enhance space connectivity, focusing on capacity, latency, and availability improvements.

1) Data Relay Systems: Despite higher path losses and latency compared to LEO, DRS in MEO and GEO offers opportunities for MCSS integration, especially for enhancing connectivity in polar and high-altitude orbits. Fig. 8 and Fig. 9 highlight capacity variations in HE and HE+ configurations. MCSS provides superior capacity for polar orbits, while MEO and GEO systems are more effective for equatorial users. Integration with MCSS can significantly boost uplink capacity and maintain consistent downlink capacity across various user altitudes.

2) System Capacity, Terminal Configuration, and User Orbits: HE configuration integration between OneWeb and O3B shows enhanced performance for polar orbit users, with OneWeb excelling up to an altitude of 800 km. Eutelsat, suited for HE+ with larger antennas, is not shown because it cannot close the link with the HE configuration. Fig. 9 compares LEO, MEO, and GEO capacities in HE+ configuration, revealing LEO's higher uplink capacity (6 Tbit) compared to MEO (3 Tbit) and GEO (0.3 Tbit).

Integrating OneWeb with Eutelsat and O3B offers varied benefits. For HE+ configurations, integration improves system availability and capacity, particularly for LEO payloads below 800 km. For HE configurations, integrating MEO (O3B) increases capacity for users with low to mid-inclinations and high altitudes, offering near-total availability and terabit-level capacity.

VII. Conclusions

This paper presented a comprehensive evaluation framework for MCSS using Monte Carlo simulations. A detailed MCSS evaluation algorithm has been presented. Four Space User Terminal (SUTs) configurations were presented, including modem, antenna, and power amplifier, demonstrating its suitability for various platforms, including small satellites. 5G

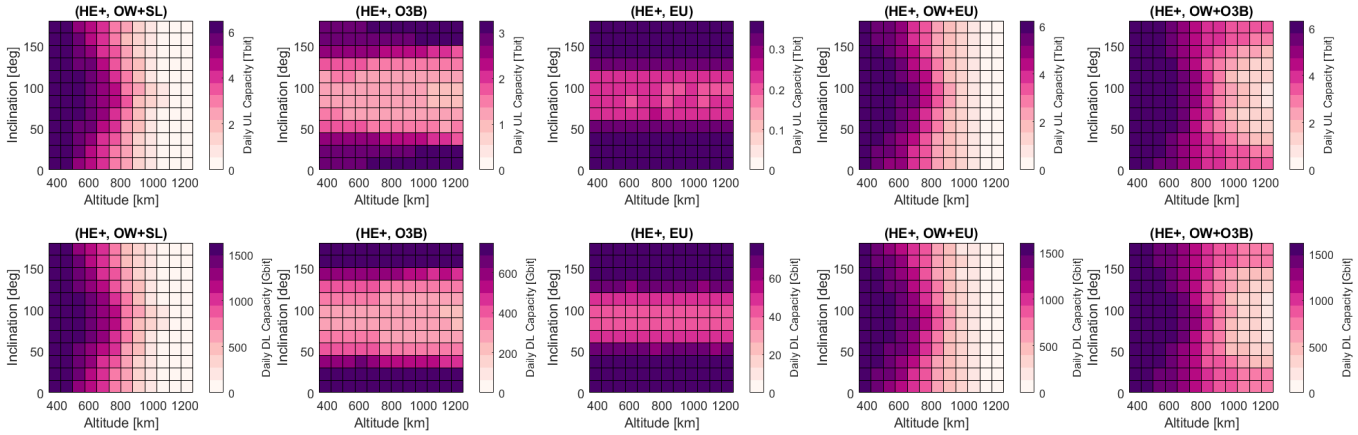

Fig. 9: MCSS capacity for HE+ configuration using multiple constellations. Left-to-right: OneWeb and Starlink (OW+SL), O3B mPOWER (O3B), OneWeb and Eutelsat (OW+EU), OneWeb and O3B mPOWER (OW+O3B). Top: UL. Bottom: DL.

New Radio Adaptive Coded Modulation has been adopted to compute the terminal capacity. Results showed that MCSS technologically surpasses existing systems in capacity and latency, especially for users in low altitudes or near critical inclinations. The presented results validate MCSS as an effective solution for transforming LEO space users into active nodes in a space internet. It offers high throughput (Tbit/day), low latency (unmatched by ground station networks), and low cost. Finally, we showed the integration of MEO/GEO DRS into MCSS, highlighting synergies and limitations for space users as 6G user equipment in NTN. These findings reveal MCSS's potential to entirely disrupt the 6G and space ecosystem. As part of the 6G framework, mega-constellations could deliver services to satellites similar to terrestrial users. Further research for future studies includes service and technical aspects like licensing, addressing, routing, compatibility, channel allocation, more sophisticated handover criteria, and interference mitigation.

VIII. Acknowledgments

The authors would like to thank Pier Bargellini and the European Space Agency for their support through ESA's Open Space Innovation Platform and different specialists at ESOC for the valuable discussions during the study. This research has also received support from the European Union's Horizon 2020 R&D program under the Marie Skłodowska-Curie grant agreement No 101008233 (MISSION project) and the French National Research Agency (ANR) under the project ANR-22-CE25-0014-01.

References

[1] M. M. Azari, S. Solanki, S. Chatzinotas, O. Kodheli, H. Sallouha, A. Colpaert, J. F. M. Montoya, S. Pollin, A. Haqiqatnejad, A. Mostaani *et al.*, "Evolution of non-terrestrial networks from 5g to 6g: A survey," *IEEE communications surveys & tutorials*, 2022.

[2] F. Rinaldi, H.-L. Maattanen, J. Torsner, S. Pizzi, S. Andreev, A. Iera, Y. Koucheryavy, and G. Araniti, "Non-terrestrial networks in 5g & beyond: A survey," *IEEE access*, vol. 8, pp. 165 178–165 200, 2020.

[3] J. A. Fraire, O. Iova, and F. Valois, "Space-terrestrial integrated internet of things: Challenges and opportunities," *IEEE Communications Magazine*, 2022.

[4] O. Kodheli, E. Lagunas *et al.*, "Satellite communications in the new space era: A survey and future challenges," *IEEE Communications Surveys & Tutorials*, vol. 23, no. 1, pp. 70–109, 2020.

[5] C. Sacchi, G. Fabrizio, M. Marchese, K. Cheung, and M. Noble, "Foreword to the Special Section on Information and Communication Technologies (ICT) for a New Space Vision," *IEEE Transactions on Aerospace and Electronic Systems*, vol. 58, no. 5, pp. 3743–3745, October 2022, doi:10.1109/TAES.2022.3209856.

[6] A. Golkar and A. Salado, "Definition of New Space—Expert Survey Results and Key Technology Trends," *IEEE Journal on Miniaturization for Air and Space Systems*, vol. 2, no. 1, pp. 2–9, March 2021, doi:10.1109/JMASS.2020.3045851.

[7] European Space Agency Debris Office, "ESA's Annual Space Environment Report," European Space Agency, Tech. Rep., 2022. [Online]. Available: https://www.sdo.esoc.esa.int/environment_report/Space_Environment_Report_latest.pdf

[8] EuroConsult, "Satellites to be built & launched by 2030 - a complete analysis & forecast of the satellite manufacturing & launch service markets," EuroConsult, Tech. Rep., 2021. [Online]. Available: https://digital-platform.euroconsult-ec.com/wp-content/uploads/2022/01/Extract_Sat_Built_2021.pdf

[9] C. Ravishankar, R. Gopal, N. BenAmmar, G. Zakaria, and X. Huang, "Next-generation global satellite system with mega-constellations," *International journal of satellite communications and networking*, vol. 39, no. 1, pp. 6–28, 2021.

[10] T. S. G. R. A. Network, "3gpp tr38.821: Solutions for nr to support non-terrestrial networks (ntn) (release 16) v16.2.0," 3rd Generation Partnership Project, Tech. Rep., 04-2023. [Online]. Available: https://www.3gpp.org/ftp/Specs/archive/38_series/38.821/38821-g20.zip

[11] F. Heine *et al.*, "The european data relay system, high speed laser based data links," in *2014 7th ASMS/SPSC*. IEEE, 2014, pp. 284–286.

[12] D. Calzolaio *et al.*, "Edrs-c–the second node of the european data relay system is in orbit," *Acta Astronautica*, vol. 177, pp. 537–544, 2020.

[13] M. Mitry, "Routers in Space: Kepler Communications' CubeSats will Create an Internet for Other Satellites," *IEEE Spectrum*, vol. 57, no. 2, pp. 38–43, February 2020, doi:10.1109/MSPEC.2020.8976900.

[14] National Aeronautics and Space Administration. Tracking and Data Relay Satellite. [Online]. Available: https://www.nasa.gov/directorates/heo/scan/services/networks/tdrs_main/

[15] B. Bag, A. Das, I. S. Ansari, A. Prokeš, C. Bose, and A. Chandra, "Performance analysis of hybrid fso systems using fso/rf-fso link adaptation," *IEEE Photonics Journal*, vol. 10, no. 3, pp. 1–17, 2018.

[16] O. B. Yahia, E. Erdogan, G. K. Kurt, I. Altunbas, and H. Yanikomeroglu, "A weather-dependent hybrid rf/fso satellite communication for improved power efficiency," *IEEE Wireless Communications Letters*, vol. 11, no. 3, pp. 573–577, 2021.

[17] K. Tekbiyik, G. K. Kurt, A. R. Ektı, and H. Yanikomeroglu, "Reconfigurable intelligent surfaces empowered thz communication in leo satellite networks," *IEEE Access*, vol. 10, pp. 121 957–121 969, 2022.

[18] Y. Xing and T. S. Rappaport, "Terahertz wireless communications: Co-sharing for terrestrial and satellite systems above 100 ghz," *IEEE communications letters*, vol. 25, no. 10, pp. 3156–3160, 2021.

[19] R. Tubío-Pardavila and N. Kurahara, "Ground station networks," in *Cubesat Handbook*. Elsevier, 2021, pp. 353–364.

[20] S. Strasser, T. Mayer-Gürr, and N. Zehentner, "Processing of gnss constellations and ground station networks using the raw observation approach," *Journal of Geodesy*, vol. 93, no. 7, pp. 1045–1057, 2019.

[21] N. J. Rattenbury, J. Ashby, F. Bennet, M. Birch, J. E. Cater, K. Ferguson, D. Giggenbach, K. Grant, A. Knopp, M. T. Knopp *et al.*, "Update on the german and australasian optical ground station networks," *arXiv preprint arXiv:2402.13282*, 2024.

[22] J. W. Cutler and A. Fox, "A framework for robust and flexible ground station networks," *Journal of Aerospace Computing, Information, and Communication*, vol. 3, no. 3, pp. 73–92, 2006.

[23] R. A. d. Carvalho, "Optimizing the communication capacity of a ground station network," *Journal of Aerospace Technology and Management*, vol. 11, p. e2319, 2019.

[24] J. Cutler, P. Linder, and A. Fox, "A federated ground station network," in *SpaceOps 2002 Conference*, 2002, p. 72.

[25] H. Al-Hraishawi, H. Chougrani, S. Kisseleff, E. Lagunas, and S. Chatzinotas, "A survey on non-geostationary satellite systems: The communication perspective," *IEEE Communnications Surveys & Tutorials*, 2022.

[26] H. Al-Hraishawi, M. Minardi, H. Chougrani, O. Kodheli, J. F. M. Montoya, and S. Chatzinotas, "Multi-layer space information networks: Access design and softwarization," *IEEE Access*, vol. 9, pp. 158 587–158 598, 2021.

[27] G. Maiolini Capez, M. Caceres, R. Armellin, C. Bridges, S. Frey, R. Garello, P. Bargellini, "Characterisation of Mega-Constellation Links for LEO Missions with Applications to EO and ISS Use Cases," *IEEE Access*, pp. 3743–3745, March 2023, doi:10.1109/ACCESS.2023.3254917.

[28] H. Chougrani, O. Kodheli *et al.*, "Connecting space missions through ngso constellations: Feasibility study," *Frontiers in Communications and Networks*, vol. 5, p. 1356484, 2023.

[29] Defense Mapping Agency, "Department of defense world geodetic system 1984," DMA, TR 8350.2, 1991. [Online]. Available: https://apps.dtic.mil/sti/pdfs/ADA280358.pdf

[30] J. Wertz, D. Everett, and J. Puschell, *Space Mission Engineering: The New SMAD*, ser. Space technology library. Microcosm Press, 2011.

[31] D. A. Vallado, *Fundamentals of astrodynamics and applications*. Springer Science & Business Media, 2001, vol. 12.

[32] SES. (2022) O3b mPOWER - A New Era of Scale, Performance, and Flexibility for Satellite Communications. [Online]. Available: https://www.ses.com/o3b-mpower

[33] ——. (2022) SES GEO HTS - Global reach with superior performance. [Online]. Available: https://www.ses.com/our-coverage/geo-hts

[34] F. Heine, G. Mühlnikel, H. Zech, S. Philipp-May, and R. Meyer, "The European Data Relay System, High Speed Laser based Data Links," in *2014 7th ASMS/SPSC*, September 2014, pp. 284–286, doi:10.1109/ASMS-SPSC.2014.6934556.

[35] S. Yamakawa, Y. Satoh, T. Itahashi *et al.*, "LUCAS: The Second-Generation GEO Satellite-based Space Data-Relay System using Optical Link," in *2022 IEEE International Conference on Space Optical Systems and Applications (ICSOS)*, March 2022, pp. 14–16, doi:10.1109/ICSOS53063.2022.9749726.

[36] C. Cicala, C. Abbundo, S. Cannavacciuolo, M. D. Graziano, V. Striano, and R. D. Prete, "A Preliminary Feasibility Analysis of a New Data-Relay Small Satellites Constellation," in *2022 IEEE 9th International Workshop on Metrology for AeroSpace (MetroAeroSpace)*, June 2022, pp. 497–502, doi:10.1109/MetroAeroSpace54187.2022.9856195.

[37] D. T. Kelso. Celestrak. [Online]. Available: https://celestrak.org/

[38] World Vu Satellites Limited, "Application for Fixed Satellite Service by WorldVu Satellites Limited, Debtor-in-Possession (SAT-MPL-20200526-00062)," World Vu Satellites Limited, Tech. Rep., 2022. [Online]. Available: https://fcc.report/IBFS/SAT-MPL-20200526-00062/

[39] Space Exploration Holdings, "Application for Fixed Satellite Service by Space Exploration Holdings, LLC (SAT-MOD-20181108-00083)," Space Exploration Holdings, Tech. Rep., 2019. [Online]. Available: https://fcc.report/IBFS/SAT-MOD-20181108-00083/

[40] International Telecommunication Union, "Satellite antenna radiation patterns for non-geostationary orbit satellite antennas operating in the fixed-satellite service below 30 GHz," International Telecommunication Union, Tech. Rep., 2001. [Online]. Available: https://www.itu.int/dms_pubrec/itu-r/rec/s/R-REC-S.1528-0-200106-I!!PDF-E.pdf

[41] G. Barue, *Satellite Communications*. John Wiley & Sons, Ltd, 2008, ch. 5, pp. 391–424. [Online]. Available: https://onlinelibrary.wiley.com/doi/abs/10.1002/9780470290996.ch5

[42] Eutelsat, "Earth Station Technical and Operational Minimum Requirements - Standard M, Issue 16 Rev.5, July 2022," Eutelsat, Tech. Rep., 2022. [Online]. Available: https://www.eutelsat.com/files/PDF/support/EESS-502.pdf

[43] N. Gatti, P. Gabellini, L. Russo, T. Waterfield, J. Hinds, S. Amos, H. Fenech, "Ku-band downlink reconfigurable active antenna for quantum mission," in *33rd AIAA International Communications Satellite Systems Conference and Exhibition*, 2015.

[44] H. Fenech, S. Amos, and T. Waterfield, "The role of array antennas in commercial telecommunication satellites," in *2016 10th European Conference on Antennas and Propagation (EuCAP)*, 2016, pp. 1–4.

[45] J. Sedin, L. Feltrin, and X. Lin, "Throughput and capacity evaluation of 5g new radio non-terrestrial networks with leo satellites," in *GLOBECOM 2020*, 2020, pp. 1–6.

[46] Intelsat, "Galaxy 30 at 125°w," Intelsat, Tech. Rep., 2020. [Online]. Available: https://www.intelsat.com/wp-content/uploads/2020/08/5533-G-30_2020-002.pdf

[47] T. E. Humphreys *et al.*, "Signal structure of the starlink ku-band downlink," *IEEE Transactions on Aerospace and Electronic Systems*, vol. 59, no. 5, pp. 6016–6030, 2023.

[48] P. S. Maybeck, *Stochastic Models, Estimation, and Control*. Academic press, 1982.

[49] R. H. David Vallado, Paul Crawford and T. Kelso, "Revisiting spacetrack report #3," in *AIAA/AAS Astrodynamics Specialist Conference and Exhibi*, 2006.

[50] N. Pachler, I. del Portillo, E. F. Crawley, and B. G. Cameron, "An Updated Comparison of Four Low Earth Orbit Satellite Constellation Systems to Provide Global Broadband," in *2021 IEEE International Conference on Communications Workshops (ICC Workshops)*, June 2021, pp. 1–7, doi:10.1109/ICCWorkshops50388.2021.9473799.

Gabriel Maiolini Capez is a PhD student in Electronics and Telecommunications Engineering at Politecnico di Torino, where he holds a Master's degree in Communications and Computer Networks Engineering. He has wide domain experience in satellite communication systems, space networks, and digital signal processing algorithms. His research focuses on innovative communication and ranging systems for space-to-space and space-to-ground applications, including constellation design.

Mauricio A. Cáceres received a Ph.D. in Electronic Engineering in 2011 from Politecnico di Torino with a thesis on Belief Propagation for Positioning, Navigation and Timing applications with Signals of Opportunity. During his doctorate, he was a visiting student at Chalmers University, Gothenburg, and Columbia University, New York. From 2007 to 2012, he was with Istituto Superiore Mario Boella (now LINKS Foundation), Turin. From 2012 to 2020, he was with the German Aerospace Centre (DLR), Oberpfaffenhofen. From 2020 to 2023, he was a Senior Systems Engineer at Vyoma GmbH, Munich, affiliation where this research was conducted. From 2024, he is a Senior Space Surveillance and Tracking Official with the European Union Agency for the Space Programme (EUSPA), Madrid. His main research topics are data fusion and machine learning applied to spaceflight dynamics and space systems engineering. On these topics he has co-authored more than 20 papers. He has been the Project Manager of several research projects, and mentored PhD and Master students alike.

Roberto Armellin graduated in 2003 with a first-class honors degree in Aerospace Engineering from Politecnico di Milano. In Milan, he began his research activity first as a Ph.D. student (2004-2007), and later (2007-2013) as a postdoctoral researcher. From 2014 to 2015, he was a lecturer in Astrodynamics at the University of Southampton, a position he left when awarded a 2-year Intra-European Marie Curie Individual Fellowship at Universidad de la Rioja. At the end of this fellowship, he joined the Surrey Space Centre at the University of Surrey as a Senior Lecturer in Spacecraft Dynamics, where he also served as Postgraduate Research Director. He spent one year as a Professor of Space Systems at ISAE-SUPAERO before joining the Te Pūnaha Ātea Auckland Space Institute in late 2020. His main interests are space situational awareness and trajectory optimization and guidance.

Chris P. Bridges received the B.Eng. degree from the Uni. of Greenwich, London, U.K., in 2005, and the Ph.D. degree from the Uni. of Surrey, Guildford, Surrey, U.K., in 2009. He leads the On-Board Data Handling (OBDH) Research Group, Surrey Space Centre (SSC), Uni. of Surrey, Guildford, U.K. He has designed, built, and operated numerous nanosat platform and payload systems and contributes toward instrument and avionics hardware and software in industry. He currently supports satellite operations and is developing systems for the ESA Volatile and Mineralogy Mapping Orbiter (ESA VMMO) Lunar Mission. His research include software-defined radios, real-time embedded systems, machine learning computing implementations, and astrodynamics computing methods.

Juan A. Fraire is a researcher at INRIA (France) and a guest professor at CONICET-UNC (Argentina) and Saarland University (Germany). Core topics of his interest are near-Earth and deep-space networking and informatics, adding up to more than 100 published papers in international journals and leading conferences. Juan is the co-founder and chair of the Space-Terrestrial Internetworking Workshop (STINT) and participates in diverse joint projects with space agencies (e.g., NASA, ESA, CONAE) and companies in the space sector (e.g., D3TN, Skyloom).

Stefan Frey received his M.S. degree in Mechanical Engineering from ETH Zurich, Switzerland in 2014. From 2015 to 2016, he worked as a Research Assistant in the Space Debris Office of the European Space Agency. Through 2017 to 2020, he concluded his PhD studies as an Aerospace Engineer at the Politecnico di Milano, Italy, focusing on the impact that orbital fragmentation events have on active satellites in terms of collision probability. Since 2020, Dr Stefan Frey is a co-founder and managing director of Vyoma GmbH, a company focused on increasing safety in space through space-based surveillance and automation services.

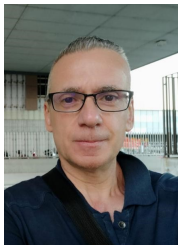

Roberto Garello received a Ph.D. in Electronic Engineering in 1994 from Politecnico di Torino with a thesis on Error Correction Coding. During his doctorate, he was a visiting student at MIT, Cambridge, and ETH, Zürich. From 1994 to 1997, he was with Marconi Communications, Genoa. From 1998 to 2001, he was an Associate Professor at the University of Ancona. From November 2001 he is an Associate Professor in the Department of Electronics and Telecommunications at Politecnico di Torino. In 2003 he was appointed Senior Member of IEEE. In 2017 he was an Adjunct Professor at California State University, Los Angeles. His main research topics are space communication systems and channel coding. On these topics, he has co-authored more than 150 papers and has been the Project Manager for over 40 research projects.